Proton Mobilities in Water and in Different Stereoisomers of Covalently Linked Gramicidin A Channels

Samuel Cukierman
Department of Physiology, Loyola University Medical Center, Maywood, Illinois 60153 USA

ABSTRACT Proton conductivities in bulk solution (λ_H) and single-channel proton conductances (g_H) in two different stereoisomers of the dioxolane-linked gramicidin A channel (the SS and RR dimers) were measured in a wide range of bulk proton concentrations ([H], 0.1–8000 mM). Proton mobilities (μ_H) in water as well as in the SS and RR dimers were calculated from the conductivity data. In the concentration range of 0.1–2000 mM, a straight line with a slope of 0.75 describes the log (g_H)-log ([H]) relationship in the SS dimer. At [H] $>$ 2000 mM, saturation is followed by a decline in g_H. The g_H-[H] relationship in the SS dimer is qualitatively similar to the [H] dependence of λ_H. However, the slope of the straight line in the log(λ_H)-log([H]) plot is 0.96, indicating that the rate-limiting step for proton conduction through the SS dimer is not the diffusion of protons in bulk solution. The significant difference between the slopes of those linear relationships accounts for the faster decline of μ_H as a function of [H] in the SS dimer in relation to bulk solution. In the high range of [H], saturation and decline of g_H in the SS dimer can be accounted for by the significant decrease of μ_H in bulk solution. At any given [H], g_H in the RR dimer is significantly smaller than in the SS. Moreover, the g_H-[H] relationship in the RR stereoisomer is qualitatively different from that in the SS. Between 1 and 50 mM [H], g_H can be fitted with an adsorption isotherm, suggesting the presence of a proton-binding site inside the pore ($pK_a \approx 2$), which limits proton exit from the channel. At 100 mM $<$ [H] $<$ 3000 mM, g_H increases linearly with [H]. The distinctive shape of the g_H-[H] relationship in the RR dimer suggests that the channel can be occupied simultaneously by more than one proton. At higher [H], the saturation and decline of g_H in the RR dimer reflect the properties of μ_H in bulk solution. In the entire range of [H], protons seem to cross the SS and RR channels via a Grotthuss-like mechanism. The rate-limiting step for proton transfer in the SS dimer is probably the membrane-channel/bulk solution interface. It is also proposed that the smaller g_H in the RR dimer is the consequence of a different organization and dynamics of the H-bonded network of water molecules inside the pore of the channel, resulting in a slower proton transfer and multiple pore occupancy by protons.

INTRODUCTION

The transfer of protons across membranes is an essential phenomenon in biology. ATP synthesis is driven by proton flow across membrane proteins. Voltage-dependent proton currents are present in many different cell types (De Coursey and Cherny, 1994, 1998) and are important in the physiology of white blood cells (De Coursey and Cherny, 1998). Proton channels have not yet been cloned (De Coursey, 1998), and the measurement of proton flow and its regulation in bioenergetic proteins cannot be approached as directly as in ion channels. Consequently, essential questions concerning how protons are transferred in proteins and how this transfer is affected by molecular manipulations of the protein have been difficult to address experimentally.

Gramicidin A (gA) is a pentadecapeptide formed by an alternating sequence of D- and L-amino acids (Sarges and Witkop, 1965). This primary structure determines a right-handed β-helix (Arseniev et al., 1985; Ketchem et al., 1997; Kovacs et al., 1999). In lipid bilayers, the establishment of six H-bonds between gA monomers localized in opposite monolayers forms an ion channel that is selective for monovalent cations only (Andersen, 1984; Busath, 1993; Cross, 1997; Koeppe and Andersen, 1996). The pore of gA channels has a single file of water molecules, and diffusion of monovalent cations occurs in a single-file or no-pass condition (Finkelstein and Andersen, 1981; Levitt, 1984). The single-channel conductance to protons (g_H) in natural gA channels is very high in relation to other monovalent cations. While gA has maximum single-channel conductances in the range of tens of pS for different monovalent cations, g_H can be one to two orders of magnitude larger (Myers and Haydon, 1972; Hladky and Haydon, 1972; Eisenman et al., 1980; Busath and Szabo, 1988). Proton conduction in solution as well as in gA channels does not occur hydrodynamically, but by a special transfer process that is known as the Grotthuss mechanism (see Discussion). In fact, Levitt et al. (1978) demonstrated that proton conduction in gA channels is not accompanied by water flow as with other monovalent cations, and this was decisive in establishing the nonhydrodynamic nature of proton conduction in gA channels.

In 1989, Stankovic and collaborators linked two gA monomers with a dioxolane group. The rationale for developing this approach was the possibility of addressing structure-function relationships in gA channels. The reason for using the dioxolane group is that in one of the dimers (the SS, see below) it provides a continuous and constrained transition between the two β-helices of gA, thus maintain-

Received for publication 9 November 1999 and in final form 18 January 2000.

Address reprint requests to Dr. Samuel Cukierman, Department of Physiology, Loyola University Medical Center, 2160 South First Ave., Maywood, IL 60153. Tel.: 708-216-9471; Fax: 708-216-6308; E-mail: scukier@luc.edu.

0006-3495/00/04/1825/10 $2.00

ing the secondary structure of gA channels. By using different stereoisomers of the dioxolane linker, two different gA dimers can be synthesized, the SS and the RR dimers (Stankovic et al., 1989; Quigley et al., 1999). The origin of the structural differences between the SS and RR dimers resides in the different chiralities of the dioxolane linker (see Quigley et al., 1999; Stankovic et al., 1989). One essential structural difference between the SS and RR dimers concerns the network of H-bonds inside the dimer. In the SS dimer, this H-bond network is similar to that in natural gA channels, while in the RR dimer it is markedly different (Crouzy et al., 1994; Quigley et al., 1999). In particular, in the middle of the RR dimer one H-bond between a Val in one gA monomer and an Ala in the other monomer cannot be formed because of a significant local distortion of the secondary structure of the protein caused by the RR dioxolane (Quigley et al., 1999). Because g_H in the SS dimer is considerably larger than in the RR dimer, it was hypothesized that differences in the energetics of H-bonds in water-water and water-channel carbonyls between different stereoisomers could explain the differences in g_H (see Discussion).

In this paper, g_H in both the SS and RR dimers were measured in a wide range of [H] (0.1–8000 mM). The single-channel conductances and the calculated proton mobilities are compared to the conductivity and mobility of protons in bulk water. Over the entire range of [H], g_H in the RR dimer is significantly smaller than in the SS. The different stereoisomers of dioxolane-linked gA channels are a powerful model for the study at the molecular level of proton transfer in proteins. The novel results presented in this study indicate that the experimental differences between g_H values in the SS and RR dimers are more diverse and interesting than previously recognized.

MATERIALS AND METHODS

Planar lipid bilayers made of glyceryl-monooleate (GMO) in decane (~60 mM) were formed onto a 0.1-mm-diameter hole in a polystyrene partition separating two solutions with identical concentrations of HCl. In contrast to phospholipid bilayers, GMO bilayers were used in the present experiments because they do not develop a positive surface potential at different [H] (Cukierman et al., 1997). The lack of a positively charged interface makes the interpretation of experimental results less complicated.

Ag/AgCl electrodes immersed in bulk solution on different sides of the bilayer were used to voltage-clamp the bilayer and record single-channel currents. Single-channel currents in response to voltage clamp ramps generated in ~7 s were recorded with an Axopatch 1D (Axon Instruments, Sunnyvale, CA). Single-channel recordings were always subtracted from currents in response to voltage ramps applied to the same membrane without the ion channel.

Different solutions were made by diluting a concentrated stock solution of HCl (Fisher Scientific Co., Chicago, IL). Previously synthesized SS or RR dimers (Cukierman et al., 1997; Quigley et al., 1999) were added to only one side of the bilayer. Identification of the incorporation of the SS or RR into the bilayer dimer was made possible by the extremely long open times of these channels in relation to natural gA (Cukierman et al., 1997; Quigley et al., 1998, 1999).

The single-channel proton conductance in the SS or RR dimer was calculated using regression analysis of the linear portion of the I_H-V_m plots (see Fig. 1). The activity coefficients used to transform proton concentrations into activities (Fig. 2) were from Robinson and Stokes (1959).

Conductivities of HCl solutions (λ_{HCl}) were measured with a YSI-3200 conductivity meter, using a cell of 10.00 cm^{-1} (Yellow Spring instruments, Yellow Springs, OH). All measurements were made at room temperature (21–23°C).

Proton conductivities (λ_H) in different solutions were calculated using the relationship

$$\lambda_H = \lambda_{HCl} \cdot t_H \quad (1)$$

where t_H (~0.84) is the transference number for protons (Lengyel et al., 1962; Robinson and Stokes, 1959). Equivalent proton mobilities in solution (μ_H) were calculated as

$$\mu_H = \lambda_H \cdot F^{-1} \cdot [H]^{-1} \quad (2)$$

where F is the Faraday constant

The mobility of a proton inside an ion channel is defined as the average drift velocity of the proton divided by the electric field across the channel:

$$\nu_H = L/\tau \cdot (V/L)^{-1} = L^2 \cdot (V \cdot \tau)^{-1} \quad (3)$$

In Eq. 3, L is the length of the dioxolane-linked gA dimers (taken as 25 Å), V is the voltage drop across the channel, and τ is the average residence time of one proton inside the channel. τ can be estimated from single-channel proton currents (I_H) as

$$\tau = e \cdot (I_H)^{-1} \quad (4)$$

where e is the elementary charge. Replacing τ in Eq. 3 leads to (Cukierman et al., 1997)

$$\nu_H = L^2 \cdot g_H \cdot e^{-1} \quad (5)$$

As [H] increases, so will λ_H and g_H. However, it is important to separate the conductivity increase due to a larger number of ions available to carry current from the efficiency with which each ion carries the current. It is customary to normalize the macroscopic measurements of conductivity or mobility by the actual proton concentration. This normalized value (equivalent mobility) provides insight into the average mobility per proton. Thus Eq. 5 is divided by [H] to give the equivalent proton mobility in gA channels:

$$\mu_H = L^2 \cdot g_H \cdot (e \cdot [H])^{-1} \quad (6)$$

It will be discussed below that a significant portion of the resistance to proton flow in the SS dimer of the dioxolane-linked gA dimer may be confined to thin (~10 Å) extrachannel regions adjacent to the mouth of the pore. Thus μ_H in the SS or RR dimer represents the average mobility of a proton crossing the membrane/bulk solution interfaces and the channel itself.

RESULTS

In Fig. 1, single-channel proton currents (in pA) in response to voltage clamp ramps (mV) are shown in different [H]. In each panel, the top and bottom recordings represent typical single-channel current recordings from the SS and RR dimers, respectively (different experiments in different GMO bilayers). Different cutoff frequencies were used in each panel (see legend). As [H] increases, g_H in both the SS and RR dimers increases. However, the rate at which g_H

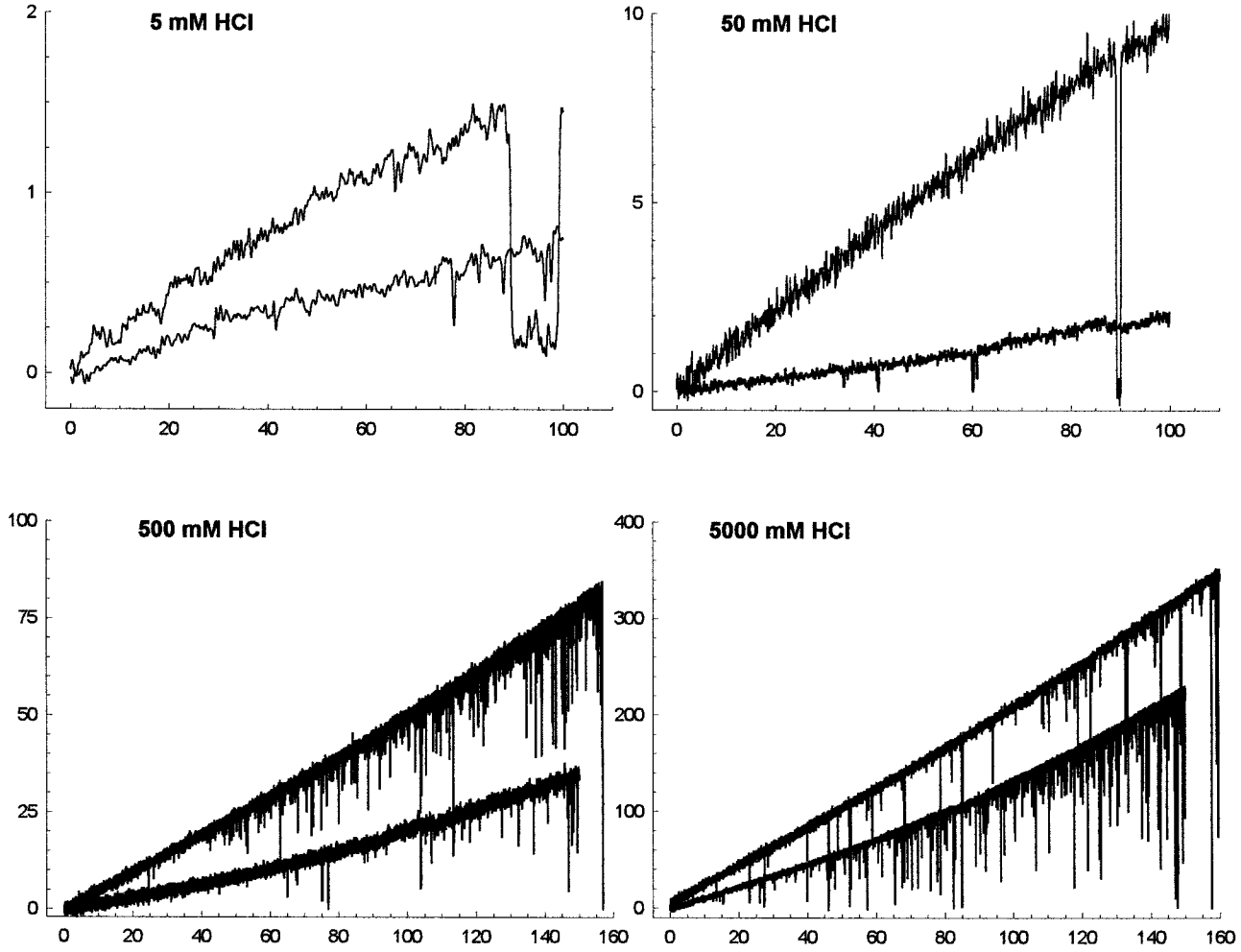

FIGURE 1 Single channel proton currents (pA) in response to voltage clamp ramps (from 0 to 100 or 160 mV) in the SS and RR dimers in different [HCl]. g_H was estimated from the initial linear portion of the current recording. g_H values were (for the SS and RR dimers, respectively) 5 mM, 20 and 8 pS; 50 mM, 104 and 17 pS; 500 mM, 495 and 171 pS; 5000 mM, 1827 and 1147 pS. Recordings were low-pass Bessel filtered at 2 kHz (500 and 5000 mM) and at 200 Hz (50 mM). In 5 mM HCl, original recordings were filtered at 100 Hz, and for the sake of clarity they were further filtered at 20 Hz, using the Bessel filter in the Clampfit software.

increases is clearly different between the different stereoisomers. In the experiments of Fig. 1, the ratios between g_H values in the SS and RR dimers are 2.5, 6.1, 2.9, and 1.6 in 5, 50, 500, and 5000 mM [H], respectively. Depending on [H], the *I-V* plots in both the SS and RR dimers show departures from linearity (sub- or supralinearity) at relatively large voltages (Cukierman et al., 1997; Quigley et al., 1999). Another consistent observation that will not be addressed here is that as [H] increases, so does the frequency of brief closures in the SS and RR dimers (Cukierman et al., 1997; Quigley et al., 1999).

In the upper panel of Fig. 2, the dependence of the linear part of g_H on [H] in the SS (*circles*) and RR (*squares*) dioxolane-linked gA dimers is shown. In the concentration range of 0.1–2000 mM, circles were fitted with a straight line with a slope of 0.75. Between the concentrations of 2000 and 6000 mM, g_H is essentially unchanged, and in 8000 mM, a decline in g_H is clearly seen. At any given [H], the single-channel proton conductance in the RR dimer is significantly smaller than in the SS. However, the g_H-[H] relationship in the RR dimers is clearly not linear as in the SS. In the concentration range of 1–50 mM HCl, points are well fitted by an adsorption isotherm,

$$g_H = g^{max} \cdot (K_D/[H] + 1)^{-1} \quad (7)$$

with g_{max} = 22.6 pS, and K_D (dissociation constant of H from a binding site inside the RR pore) = 9.8 mM corresponding to a pK_a of 2 (see Fig. 3). In the concentration range of 100 mM < [H] < 3000 mM, there is a linear dependence of g_H on [H] (slope = 0.95). At [H] > 3000 mM, g_H does not increase as steeply with [H], and in 8000 mM, g_H declines as in the SS dimer. In the bottom panel of Fig. 2, proton conductivities were plotted against proton

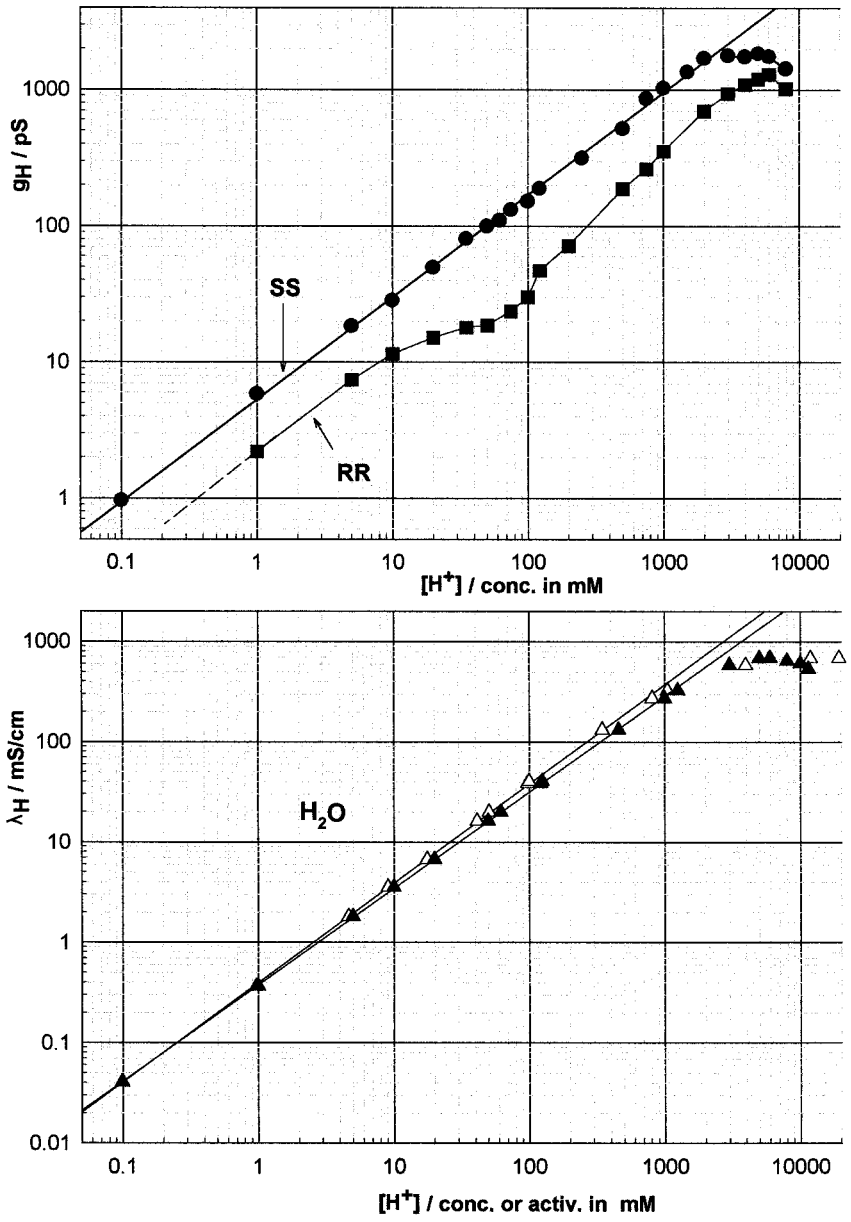

FIGURE 2 g_H-[H] plots of the SS (●) or RR (■) dimers. Each point is the mean ± SEM of 4–20 different observations (different SS channels in different or in the same GMO membrane). Error bars are smaller than the symbols. The lower graph shows proton conductivities versus [H]. ▲, △, Proton concentrations and activities, respectively.

concentration (*filled triangles*) or proton activity (*empty triangles*). Linear regression analysis in the proton concentration range of 0.1–1250 mM yielded a slope of 0.96 (*filled triangles*) or 1.00 (*empty triangles*). At [H] > 3000 mM, saturation and attenuation of λ_H occur.

The plots in Fig. 2 measure the total conductivity of a solution or an ion channel as a function of [H]. Proton conductivity is a function of the total number of protons in solution and their average mobilities. To estimate the average mobility of a proton, the single-channel conductances and bulk conductivity in Fig. 2 were translated into equivalent proton mobilities (μ_H) and plotted in Fig. 4 (see Materials and Methods). Two reference dotted lines are also shown in Fig. 4. They allow a comparison between experimental data and proton mobility due to hydrodynamic flow in bulk solution. The upper dotted line is the hydrodynamic mobility of $(H_3O)^+$ calculated from the self-diffusion coefficient of H_2O ($D_w = 2.25 \times 10^{-5}$ cm^2/s; Eisenberg and Kauzmann, 1969). This can be considered an upper limit for the hydrodynamic mobility of $(H_3O)^+$. The bottom dotted line is the measured hydrodynamic mobility of protons in a 10 M HCl aqueous solution ($\sim 0.56 \times 10^{-3}$ cm^2/(V·215·s)), using an isotopic technique (Dippel and Kreuer, 1991). Several novel features are now reported in relation to Fig. 4: 1) In 0.1 mM HCl, μ_H in water is about the same as in the SS dimer. 2) However, μ_H in the SS declines considerably and significantly faster with [H] than in water. A 50% reduction in μ_H in H_2O occurs when [HCl] increases from

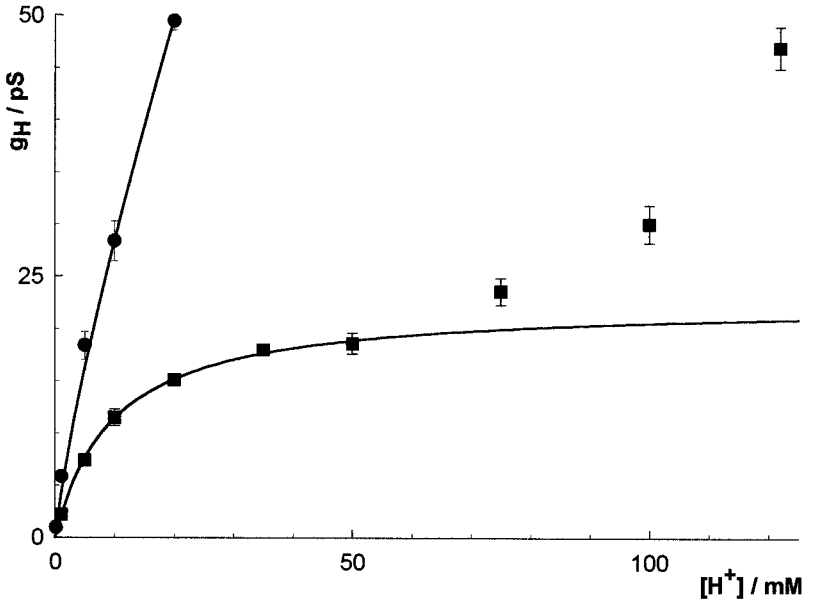

FIGURE 3 g_H-[H] relationships in the proton concentration range of 0–120 mM for the SS (●) and RR (■) dimers. Lines were drawn according to Eq. 4 (■) and $g_H = 4.4 \cdot [H]^{0.75}$ (●).

0.1 to ~2500 mM. In contrast, the same attenuation of μ_H in the SS dimer requires an increase in [HCl] from 0.1 to ~2 mM only. This is a consequence of the considerably smaller slope of the g_H-[H] relationship in relation to λ_H-[H]. 3) At [H] > 2000 mM, the rate of decline of μ_H in water has approximately the same steepness as in the SS dimer. The attenuation of μ_H in the RR dimer in that concentration range is present but is less steep than in water or the SS. 4) Not only is the μ_H in the RR dimer significantly less than in the SS dimer, but the shapes of the μ_H-[H] plots are also different. Notice that in the concentration range of 100-2000 mM, μ_H remains essentially constant for the RR dimer.

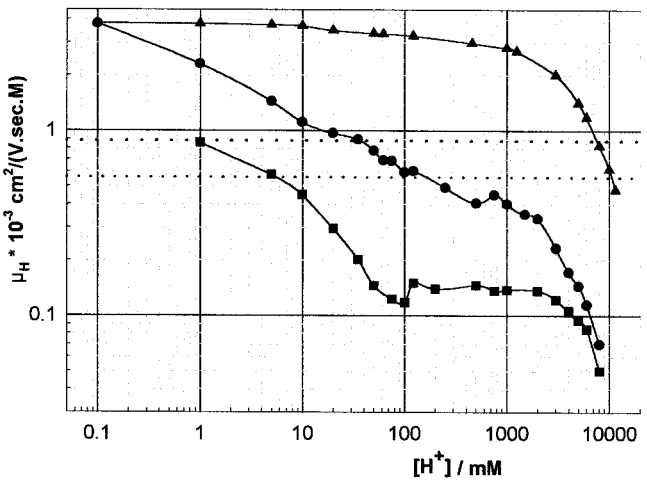

FIGURE 4 μ_H-[H] relationships for the SS (●), RR (■), and bulk solution (▲). The lines connecting the experimental points have no theoretical meaning. Two dotted lines are shown in this graph. The upper one is the proton mobility, calculated assuming hydrodynamic flow of $(H_3O)^+$ by using the self-diffusion coefficient of H_2O. The bottom dotted line is the measured μ_H in 10 M HCl (see text).

DISCUSSION

The novel experimental findings in this study are as follows: 1) In the SS dioxolane-linked gramicidin A channels, there is a linear relationship between g_H and [H] over a very wide range of concentrations (0.1–2000 mM). In a log-log plot, the slope of this line is 0.75, which is significantly different from that in water (0.96). 2) At [H] > 2000 mM, saturation followed by a significant attenuation in g_H and λ_H was demonstrated. 3) In the RR dimer, g_H is significantly smaller than in the SS dimer. Most notably, the qualitative nature of the g_H-[H] relationship in the RR dimer is different from that in the SS. In the [H] range of 0.1–100 mM, g_H does not change linearly with [H]. Instead, those points are well fitted by a simple adsorption isotherm (Fig. 3). In the range of 100-3000 mM, a linear relationship with a slope of 0.95 was found, and for [H] > 3000 mM, saturation is followed by a relatively slight decline in g_H. 4) Proton mobilities in both covalently linked gA dimers are markedly different from those in bulk solution at different [H].

The conduction of protons between electrodes located on different sides of a single channel occurs through different phases: bulk solutions, interfaces between the membrane/channel and bulk phases, and inside the ion channel itself. Because proton permeation in gA is very high, the extra-channel component of the resistance to proton flow has to be considered for the proper evaluation of g_H. In Section 1 below the basic properties of proton conduction in bulk water will be discussed. The conduction of protons in special water structures (water wires) will be analyzed in Sec-

tion 2. Section 3 examines the properties of water adjacent to the channel/membrane as studied with computational techniques. In Section 4, some possible mechanisms that could account for the experimental results presented in this study will be discussed.

1. Proton conduction in bulk water

The mobility of protons in water is "abnormally" high. While the hydrated radius of $(H_3O)^+$ is about the same as that of K^+ (2.8 versus 3.3 Å), the equivalent mobility of protons in dilute aqueous solutions is almost five times that of K^+ (3.62×10^{-3} versus 0.75×10^{-3} $cm^2/(V \cdot s)$; see Fig. 4). At low acid concentrations, proton mobility is not a function of the hydrodynamic flow of $(H_3O)^+$ (Fig. 4). This high proton mobility has attracted the attention of many investigators, and since early this century, proton transfer in water has been thought of as a two-step process (Danneel, 1905; Hückel, 1928; Bernal and Fowler, 1933; Conway et al., 1956; Lengyel and Conway, 1983; Nagle and Tristam-Nagle, 1983). In the first step, one proton hops between two water molecules (propagation of an ionic defect). This transfer is a consequence of breaking one OH covalent bond in a water molecule and reforming the covalent bond with a different proton. This occurs sequentially in a chain of water molecules, resulting in a complete reorganization of the H-bond network inside that chain (see, for example, figure 6 in Phillips et al., 1999). If successive proton transfers are to follow in the same direction, the original H-bond network in the water chain has to be restored. Thus the second step involves the structural reorientation of water molecules priming the original H-bond network (propagation of a turning defect, or structural diffusion) for the next H^+ transfer.

Historically, the rate-limiting step in proton mobility has been linked to structural diffusion. This diffusion would consist of concerted rotations of water molecules in a chain. In bulk water, however, the rate-limiting step of proton mobility is not related to water rotation as originally thought (Bernal and Fowler, 1933; Conway et al., 1956). The temperature dependence of water rotation time is different from the proton hopping time (Agmon, 1996). It has been proposed that the rate-limiting step in proton transfer in bulk water is the result of the disruption of one H-bond between two water molecules, each located in the second and first solvation shells of $(H_3O)^+$ (Agmon, 1995, 1996; Tuckerman et al., 1995). Molecular dynamics simulations of a cluster of water molecules revealed a continuous fluctuation between $(H_5O_2)^+$ and $(H_9O_4)^+$ structures. In fact, it was demonstrated that the two proton complexes occur with approximately the same probability (Tuckerman et al., 1995), suggesting that these structures are approximately isoenergetic. This would explain why proton transfer in bulk water is so fast. The sequence of events leading to proton transfer between bulk water molecules would be as follows: 1) the proton resides in the middle of an $(H_9O_4)^+$ cation (Eigen cation), i.e., one $(H_3O)^+$ surrounded by three water molecules (first solvation shell); 2) one H-bond between a water molecule in the $(H_9O_4)^+$ and another water molecule outside that complex is broken; 3) this causes a fine electrostatic imbalance that pulls the proton to an equilibrium position between two water molecules forming the complex $(H_5O_2)^+$ (Zundel cation); 4) one H-bond between two water molecules outside the $(H_5O_2)^+$ complex is broken and reformed with $(H_5O_2)^+$, leading to a final proton hop. By the end of this sequence of events, the proton would have hopped by ~2.5 Å, and the $(H_9O_4)^+$ complex is restored. The essence of fast proton hop in water is the consequence of the low energetic cost of interconversion between $(H_5O_2)^+$ and $(H_9O_4)^+$. This is caused by cleavage and reformation of two H-bonds with an activation energy of 2.6 kcal/mol (see scheme 11 in Agmon, 1996, and figure 1 in Tuckerman et al., 1995, for a geometric picture of this process).

Recent studies using quantum dynamics calculations describe a picture that is different from the classical model discussed above. In particular, it has been argued that 1) the prevalent structure of an excess proton in water is $(H_5O_2)^+$, and not $(H_9O_4)^+$, and 2) proton transfer in water occurs by a diffusion of an $O\text{-}H^+ \rightarrow O$ bond inside the H-bonded network of water molecules (Vuilleumier and Borgis, 1998, 1999). In both quantum and classical models of proton transfer in bulk water, solvent fluctuation and reorganization of H-bonds cause proton transfer, and the separation of the hop from the turn step is not as evident as in water wires (see Section 2).

Irrespective of the debate between classical and quantum views of proton transfer in water, it is clear that one significant consequence of the proposed models above is that changes in solution that cause an energetic imbalance between different forms of protonated water ($(H_5O_2)^+$, $(H_9O_4)^+$, or $(H_3O)^+$) will have the necessary effect of decreasing the mobility of protons. Of particular interest to this study is the fact that the structures of solvated H^+ and Cl^- change as a function of [HCl]. As [HCl] increases, new H-bonds between Cl and H will be formed, the H-bond between $(H_3O)^+$ and the closest water molecule will shorten, the numbers of solvation shells of $(H_3O)^+$ will decrease, and other structural details will emerge that together define a different solution structure and will ultimately decrease proton mobility (Agmon, 1998; Kameda and Uemura, 1992; Kameda et al., 1998; Dippel and Kreuer, 1991). In particular, it has been proposed that in high [HCl] the favored proton species is $(H_5O_2)^+$, and this will abolish the high proton mobility observed in dilute HCl solutions (Agmon, 1998). At high concentrations of HCl, proton mobility becomes closer or equal to the mobility of Cl^- (Agmon, 1998; Lengyel et al., 1962; Lown and Thirsk, 1971a,b; Owen and Sweeton, 1941).

Despite the progress of ideas regarding proton mobility that has occurred in the last decade, the interpretation of classical electrochemical data (λ_H, μ_H, *triangles* in Fig. 2 and 4) in water is by no means quantitative and remains essentially qualitative. In the range of 0.1 mM $<$ [H] $<$ 1000 mM, λ_H varies linearly with [H] with a slope of 0.96 ($\sim$1.00 if activities are used instead of concentrations; see Fig. 2). μ_H in that concentration range declines by $\sim$25%. For [H] $>$ 1000 mM saturation and decline in λ_H occur. This results in a fast and significant attenuation of μ_H at that high end of HCl concentrations (Fig. 4). From the discussion above, the μ_H-[H] relationship has to reflect a progressive change in the qualitative nature of proton transfer in solution. At low concentrations, μ_H is essentially determined by a Grotthuss-like mechanism discussed above, and in the high concentration range, the hydrodynamic flow of $(H_3O)^+$ will determine μ_H. It is reasonable to assume that between these limits, the two proton transfer mechanisms will be operating with different proportions.

2. Proton conduction in water wires

The arrangement of a H-bonded network of water molecules in a cable-like structure (water wires; Nagle and Morowitz, 1978) is of particular relevance to bioenergetics and ion channel biophysics. Chains of H-bonded water molecules in proteins have been demonstrated in the photosynthetic reaction center (Baciou and Michel, 1995), and in cytochrome *c* (Riistma et al., 1997) and *f* (Martinez et al., 1966) oxidases. The pore of gramicidin A is filled with water (Finkelstein and Andersen, 1981; Levitt, 1984), and this ion channel has been used in both theoretical (Pomès and Roux, 1996b) and experimental (Akeson and Deamer, 1991; Busath and Szabo, 1988; Cukierman, 1999; Cukierman et al., 1997; Quigley et al., 1998, 1999; Phillips et al., 1999) research as a model for the conduction of protons in water wires in proteins. Consequently, it is of special interest and relevance to our experimental results to discuss how protons can be transferred in one-dimensional systems.

Apolar wires

Proton transfer in an isolated system consisting of a number of water molecules aligned in a one-dimensional configuration has been studied by the use of molecular dynamics simulations (Pomès, 1999; Pomès and Roux, 1996a, 1998). These systems are known as apolar channel (or water) wires. The geometrical confinement of H_2O molecules in an apolar wire demands that the coordination number of H_2O be 2 instead of 4 (as in bulk water). One water molecule can form at most two H-bonds, one with each adjacent H_2O. Functional differences in proton transfer between bulk and water chains is a consequence of different coordination numbers. In apolar water chains, proton hopping between adjacent water molecules is an activationless process occurring on the subpicosecond time scale as in bulk water. Quantum effects in proton transfer in water wires are not as dominant as in bulk water (Pomès and Roux, 1996a, 1998; Vuilleumier and Borgis, 1998, 1999). As for the turning step (structural diffusion), the energetic cost of inverting the total dipole moment of a chain of water molecules in the absence of an excess proton depends on the number of water molecules, increasing from 0.5 (two waters) to $\sim$5.5 kcal/mol (eight waters; Pomès, 1999). Each water molecule added to the apolar wire can be expected to cause a four to fivefold attenuation of the reorientation rate constant of water molecules. This has significant consequences for H^+ conduction because wire conductivity should drop exponentially with the length of the water chain. Thus structural diffusion is the rate-limiting step in proton transfer in apolar water wires.

Polar wires: the case of gramicidin A channels

The insertion of an apolar water wire into the lumen of a gA channel redefines the structure of the water wire. Now at least one H-bond can be donated from H_2O to a carbonyl group that lines the pore, increasing the water coordination number from 2 to 3. This causes a more dynamic and interesting situation in which interruptions of the H-bond network inside the water chain can be caused by one or more water molecules each donating two H-bonds to carbonyls. This will have the effect of interrupting proton flow inside the channel (Pomès, 1999). In fact, if electrostatic interactions between waters and the channel wall are abolished, proton transfer becomes considerably faster (Pomès and Roux, 1996b). In particular, proton transfer along the entire length of the channel is now seen at the picosecond time scale. Proton transfer between adjacent water molecules in gA channels occurs in the subpicosecond time scale, and the slow reorientation step is also the rate-limiting step for proton transfer (Akeson and Deamer, 1991; Pomès and Roux, 1996b, 1998).

3. Proton conduction at the membrane/solution interface

The organization of water molecules adjacent to an hydrophobic interface is different from that in bulk (Breed et al., 1996; Israelachvili, 1992, and references therein; Lee et al., 1984; Sansom et al., 1996). Because proton transfer clearly depends on water structure (see above), the lack of information on the structure and properties of bulk solution/membrane channel interfaces makes the interpretation of g_H in the SS or RR dimers in terms of its intrinsic (channel) and access components a major challenge (Quigley et al., 1998). It has been proposed (Decker and Levitt, 1988; Levitt and Decker, 1988) that most of the resistance to proton flow in natural gA channels is determined by the access resistance of the channel. Chiu et al. (1999a,b) estimated that $\sim$90% of

the resistance to water diffusion between bulk phases on both sides of the gA channel is due to water diffusion across thin (~8 Å) regions adjacent to the mouths of the pore, while the diffusion coefficient of water inside the channel is about the same as that in bulk water. It is reasonable to assume that the same forces that retard the diffusion of water are also involved in hampering the reorientation step of water in the transfer of protons. Thus water permeability and proton conduction across gA channels are largely limited by the resistance outside the pore (Chiu et al., 1999b; Dani and Levitt, 1981; Levitt and Decker, 1988).

4. Proton conduction in the SS and RR dimers

SS versus H_2O

$0.1 \leq [H] \leq 2000$ mM. There is a remarkable qualitative similarity between the shapes of the curves relating g_H in the SS dimer and λ_H in bulk water to [H]. However, the linear regions of these two curves in log-log plots have different slopes. In a channel that does not offer a significant resistance to ion flow (diffusion limited process), g_H would be determined by

$$g_H = 2 \cdot \pi \cdot r \cdot F \cdot \mu_H \cdot [H] \quad (8)$$

where $2\pi r$ is a factor related to the geometry of the channel mouths in one dimension (in this case a hemisphere with a capture radius r; see Andersen, 1983; Decker and Levitt, 1988; Lauger, 1976). Equation 5 predicts the log-log plot of g_H-[H] to be a straight line with unitary slope. This was clearly obtained in bulk solution (when proton activities were used). However, in the SS dimer that slope is 0.75 (or 0.78 if proton activities are used instead of concentrations; results not shown). Consequently, the conduction of protons through the SS channel is not limited by proton diffusion in bulk water. This is an important and radically new conclusion, because in previous studies with different proton transporters and in a limited range of proton concentrations (see De Coursey and Cherny, 1994, 1999), it has been concluded that proton conduction was limited by diffusion in bulk water. The difference between proton transfer in different transporters was then attributed to geometrical differences in the capture radii of those proteins. A significant advancement in relation to previous work is that the experimental measurements in this study have covered a wide range of [H]. Thus proton diffusion in the SS channel is limited either by the thin bulk solution/channel interfaces, or by the channel itself. Following the discussion in Section 3, it is likely that the major limiting step in proton conduction in the SS dimer is located at the interface membrane channel/bulk solution. The (power) dependence of g_H on $[H]^{0.75}$, however, is quite intriguing and cannot be explained at present. It will be essential to study proton transfer along a thin layer of water molecules adjacent to the channel/membrane by computational techniques. This is especially important in view of the fact that Phillips et al. (1999) have demonstrated clear and significant interfacial dipole potential effects on proton conduction in gA channels.

Saturation and decay of g_H ([H] > 2000 mM). In this concentration range, the saturation and decline in g_H of the SS dimer can be understood by changes in the λ_H in bulk phases. The ratio between g_H measured at 5000 mM and the value obtained by extrapolation of the straight line to 5000 mM (Fig. 2) is 0.53. This agrees well with that same ratio calculated for λ_H (0.57) (see also De Coursey and Cherny, 1999). The drop in the μ_H-[H] relationship in this [H] range has approximately the same steepness in bulk water and the SS dimer. In this high range of [HCl], the hydrodynamic diffusion of $(H_3O)^+$ in bulk water becomes significant, and eventually the dominant form of proton transport (see Section 1 above). This will have the effect of decreasing the supply of protons to the SS channel and decreasing the diffusion of protons away from the channel-membrane/solution interface, both factors limiting g_H. While the mechanism by which proton diffuses in the interfaces (hydrodynamic or Grotthuss-like mechanism?) is unknown, it is not likely that $(H_3O)^+$ is moving hydrodynamically inside the SS pore over the entire range of [H]. It has been proposed (Dani and Levitt, 1981; Finkelstein and Andersen, 1981) that the rate of translocation of Na^+ in gA is essentially limited by the translocation of water molecules in the single-file regime. Therefore, if $(H_3O)^+$ were crossing the channel, a g_H two to three orders of magnitude smaller (closer to g_{Na}) than what is actually measured would be expected.

SS versus RR dimer

It was previously demonstrated in 1 M [H] only that g_H in the RR dimer is significantly smaller than in the SS (Quigley et al., 1999). It was proposed (see Section 2) that different g_H values could result from differences in interaction between H_2O and carbonyls in the wall of the channels. Stronger H-bonds, and/or possibly a larger number of H-bonds between water molecules and carbonyls in the RR in relation to the SS, could account for a lower g_H in the RR dimer by restraining the structural diffusion step in the polar water wire (Quigley et al., 1999). While measurements in this study of g_H in the SS and RR dimers in a wide range of [H] support this hypothesis, differences in g_H between the two stereoisomers are more complex than previously thought.

The shape of the g_H-[H] relationship in the RR dimer is characteristic of an ion channel working in a regime of double occupancy (see, for example, figure 3B in Hille and Schwarz, 1978). The g_H-[H] relationship for the RR dimer is similar to that found in natural gA channels (Eisenman et al., 1980). Recently, Schumaker et al. (1999, 2000a,b) incorporated the potentials of mean force for an excess proton and for a defect in the polar water wire in gA channels into

a stochastic model. g_H values were fitted with a model that takes into account double occupancy of the pore by protons. Proton conduction in the channel (at [H] $<$ 3000 mM) would be a consequence of the interplay between proton binding to the channel pore (limiting the exit rate) and an increased exit rate due to electrostatic repulsion between two protons inside the pore (Hille and Schwarz, 1978; Eisenman et al., 1980; Schumaker et al., 2000b). In [H] $>$ 3000 mM, our experimental results indicate that attenuation in λ_H limits the supply of protons to (and the diffusion away from) the RR channel, thus decreasing g_H.

As pointed out by De Coursey and Cherny (1999), the presence of a second proton in a polar water wire may cause the hydrogens of two adjacent water molecules to face each other (Bjerrum "D" defect; see their figure 2). Once one proton leaves the channel, a reorientation step (necessary to eliminate the Bjerrum "D" defect), that does not normally exist in a singly occupied proton channel (Pomès and Roux, 1996b), will have to occur before proton transfer resumes. This reorientation step involving a few water molecules in the wire could cause a decreased g_H in the polar water wire in a double-occupancy regime in relation to a singly occupied pore. Thus it is possible that double occupancy of the pore by protons in itself contributed to the smaller g_H in the RR dimer in relation to the SS.

CONCLUSION

In the SS dimer the conduction of protons is not limited by diffusion in bulk solution. It is possible that the main diffusion limitation step is located in the layer of water molecules adjacent to the membrane-channel interface. In the RR dimer, the experimental results suggest double occupancy of the pore by protons. Therefore, the main difference between the SS and RR dimers is apparently a shift in the rate-limiting step for proton transfer from the bulk solution/membrane interface to inside the ion channel. This is likely to be caused by major differences in the organization and dynamics of water wires inside the pores of the SS and RR dimers. In particular, a stronger H-bond interaction between waters and channel wall would contribute to attenuation of g_H in the RR dimer. Proton conduction inside the SS and RR dimers is likely to occur via a Grotthuss mechanism over a wide range of [H]. An interesting final observation is that while g_H values are about the same in the SS dimer and in natural gA channels (Cukierman et al., 1997), similar g_H-[H] relationships are shared between the RR and gA channels.

I wish to thank Drs. Thomas E. De Coursey, Régis Pomès, and Mark F. Schumaker for commenting on a previous version of this paper, and for stimulating discussions.

REFERENCES

Agmon, N. 1995. The Grotthuss mechanism. *Chem. Phys. Lett.* 244: 456–462.

Agmon, N. 1996. Hydrogen bonds, water rotation and proton mobility. *J. Chim. Phys.* 93:1714–1736.

Agmon, N. 1998. Structure of concentrated HCl solutions. *J. Phys. Chem.* 102:192–199.

Akeson, M., and D. W. Deamer. 1991. Proton conductance by the gramicidin water wire. Model for proton conductance in the F_0F_1ATPases? *Biophys. J.* 60:101–109.

Andersen, O. S. 1983. Ion movement through gramicidin A channels. Studies on the diffusion-controlled association step. *Biophys. J.* 41: 147–165.

Andersen, O. S. 1984. Gramicidin channels. *Annu. Rev. Physiol.* 46: 531–548.

Arseniev, A. S., I. L. Barsukov, V. F. Bystrov, A. L. Lonize, and Y. A. Ovchinikov. 1985. Proton NMR study of gramicidin A transmembrane ion channel. Head-to-head right handed, single stranded helices. *FEBS Lett.* 186:168–174.

Baciou, L., and H. Michel. 1995. Interruption of the water chain in the reaction center from rb. sphaeroides reduces the rate of the proton uptake and of the second electron transfer to Q B. *Biochemistry.* 34: 7967–7972.

Bernal, J. D., and R. H. Fowler. 1933. A theory of water and ionic solution, with particular reference to hydrogen and hydroxyl ions. *J. Chem. Phys.* 1:515–548.

Breed, J., R. Sankararamakrishnan, I. D. Kerr, and M. S. P. Sansom. 1996. Molecular simulations of water within models of ion channels. *Biophys. J.* 70:1643–1661.

Busath, D. D. 1993. The use of physical methods in determining gramicidin channel structure and function. *Annu. Rev. Physiol.* 55:473–501.

Busath, D. D., and G. Szabo. 1988. Permeation and characteristics of gramicidin conformers. *Biophys. J.* 53:697–707.

Chiu, S. W., S. Subramaniam, and E. Jakobsson. 1999a. Simulation study of a gramicidin/lipid bilayer system in excess water and lipid. I. Structure of the molecular complex. *Biophys. J.* 76:1929–1938.

Chiu, S. W., S. Subramaniam, and E. Jakobsson. 1999b. Simulation study of a gramicidin/lipid bilayer system in excess water and lipid. II. Rates and mechanisms of water transport. *Biophys. J.* 76:1939–1950.

Conway, B. E., J. O'M. Bockris, and H. Linton. 1956. Proton conductance and the existence of the H_3O^+ ion. *J. Chem. Phys.* 24:834–852.

Cross, T. A. 1997. Solid-state nuclear magnetic resonance characterization of gramicidin channel structure. *Methods Enzymol.* 289:672–696.

Crouzy, S., T. B. Woolf, and B. Roux. 1994. A molecular dynamics study of gating in dioxolane-linked gramicidin A channels. *Biophys. J.* 67: 1370–1386.

Cukierman, S. 1999. Flying protons in linked gramicidin A channels. *Isr. J. Chem.* 39:419–426.

Cukierman, S., E. P. Quigley, and D. S. Crumrine. 1997. Proton conduction in gramicidin A and in its dioxolane-linked dimer in different lipid bilayers. *Biophys. J.* 73:2489–2502.

Dani, J. A., and D. G. Levitt. 1981. Water transport and ion-water interaction in the gramicidin channel. *Biophys. J.* 35:501–508.

Danneel, V. H. 1905. Notiz über ionengeschwindigkeiten. *Z. Elektrochem.* 11:249–252.

Decker, E. R., and D. G. Levitt. 1988. Use of weak acids to determine the bulk limitation of H^+ ion conductance through the gramicidin channel. *Biophys. J.* 53:25–32.

De Coursey, T. E. 1998. Four varieties of voltage-gated proton channels. *Front. Biosci.* 3:477–482.

De Coursey, T. E., and V. V. Cherny. 1994. Voltage-activated hydrogen ion currents. *J. Membr. Biol.* 141:203–223.

De Coursey, T. E., and V. V. Cherny. 1998. Temperature dependence of voltage-gated H^+ currents in human neutrophils, rat alveolar epithelial cells, and mammalian phagocytes. *J. Gen. Physiol.* 112:503–522.

De Coursey, T. E., and V. V. Cherny. 1999. An electrophysiological comparison of voltage-gated proton channels, other ion channels, and other proton channels. *Isr. J. Chem.* 39:409–418.

Dippel, Th., and K. D. Kreuer. 1991. Proton transport mechanism in concentrated aqueous solutions and solid hydrates of acids. *Solid State Ionics.* 46:3–9.

Eisenberg, D., and W. Kauzmann. 1969. The Structure and Properties of Water. Oxford University Press, New York.

Eisenman, G., B. Enos, J. Hägglund, and J. Sandblom. 1980. Gramicidin A as an example of a single filing ionic channel. *Ann. N.Y. Acad. Sci.* 329:8–20.

Finkelstein, A., and O. S. Andersen. 1981. The gramicidin A channel: a review of its permeability characteristics with special reference to the single-file aspect of transport. *J. Membr. Biol.* 39:155–171.

Hille, B., and W. Schwarz. 1978. Potassium channels as multi-ion single-file pores. *J. Gen. Physiol.* 72:409–442.

Hladky, S. B., and D. A. Haydon. 1972. Ion transfer across lipid membranes in the presence of gramicidin A. I. Studies of the unit conductance channel. *Biochim. Biophys. Acta.* 274:294–312.

Hückel, H. E. 1928. Theorie der beweglichkeiten des wasserstoff- und hydroxylions in wässriger lösung. *Z. Elektrochem.* 34:546–562.

Israelachvili, J. 1992. Intermolecular and Surface Forces. 2nd ed. Academic Press, New York.

Kameda, Y., and O. Uemura. 1992. The intramolecular structure of oxonium ion in concentrated aqueous deuterochloric acid solutions. *Bull. Chem. Soc. Jpn.* 65:2021–2028.

Kameda, Y., T. Usuki, and O. Uemura. 1998. Neutron diffraction studies on the hydrogen-bonded structure in concentrated aqueous hydrochloric acid solutions. *Bull. Chem. Soc. Jpn.* 71:1305–1313.

Ketchem, R. R., B. Roux, and T. A. Cross. 1997. High-resolution polypeptide structure in a lamellar phase lipid environment from solid state NMR derived constraints. *Structure.* 5:1655–1669.

Koeppe, R. E., II, and O. S. Andersen. 1996. Engineering the gramicidin channel. *Annu. Rev. Biophys. Biomol. Struct.* 25:231–258.

Kovacs, F., J. Quine, and T. A. Cross. 1999. Validation of the single-stranded channel conformation of gramicidin A by solid-state NMR. *Proc. Natl. Acad. Sci. USA.* 96:7910–7915.

Lauger, P. 1976. Diffusion-limited ion flow through pores. *Biochim. Biophys. Acta.* 455:493–509.

Lee, C. Y., J. A. McCammon, and P. J. Rossky. 1984. The structure of liquid water at an extended hydrophobic surface. *J. Chem. Phys.* 80: 4448–4455.

Lengyel, S., and B. E. Conway. 1983. Proton solvation and proton transfer in chemical and electrochemical processes. *In* Comprehensive Treatise of Electrochemistry. B. E. Conway, J. O'M. Bockris, and E. Yeager, editors. Plenum Press, New York. 339–398.

Lengyel, S., J. Giber, and J. Tamás. 1962. Determination of ionic mobilities in aqueous hydrochloric acid solutions of different concentration at various temperatures. *Acta Chim. Hung.* 32:429–436.

Levitt, D. G. 1984. Kinetics of movement in narrow channels. *Curr. Topics Membr. Transp.* 21:181–197.

Levitt, D. G., and E. R. Decker. 1988. Electrostatic radius of the gramicidin channel determined from voltage dependence of H^+ ion conductance. *Biophys. J.* 53:33–38.

Levitt, D. G., S. R. Elias, and J. M. Hautman. 1978. Number of water molecules coupled to the transport of sodium, potassium, and hydrogen ions via gramicidin nonactin or valinomycin. *Biochim. Biophys. Acta.* 512:436–451.

Lown, D. A., and H. R. Thirsk. 1971a. Proton transfer conduction in aqueous solution. Part 1. Conductance of concentrated aqueous alkali metal hydroxide solutions at elevated temperatures and pressures. *Trans. Faraday Soc.* 67:132–148.

Lown, D. A., and H. R. Thirsk. 1971b. Proton transfer conduction in aqueous solution. Part 2. Effect of pressure on the electrical conductivity of concentrated orthophosphoric acid in water at 25°C. *Trans. Faraday Soc.* 67:149–152.

Martinez, S. E., D. Huang, M. Ponomarev, W. A. Cramer, and J. L. Smith. 1966. The heme redox center of chloroplast cytochrome *f* in linked to a buried 5-water chain. *Protein Sci.* 5:1081–1092.

Myers, V. B., and D. A. Haydon. 1972. Ion transfer across lipid membranes in the presence of gramicidin A. *Biochim. Biophys. Acta.* 274:313–322.

Nagle, J. F., and H. J. Morowitz. 1978. Molecular mechanisms for proton transport in membranes. *Proc. Natl. Acad. Sci. USA.* 75:298–302.

Nagle, J. F., and S. Tristam-Nagle. 1983. Hydrogen bonded chain mechanisms for proton conduction and proton pumping. *J. Membr. Biol.* 74:1–14.

Owen, B. B., and F. H. Sweeton. 1941. The conductance of hydrochloric acid in aqueous solutions from 5° to 65°. *J. Am. Chem. Soc.* 63: 2811–2817.

Phillips, L. R., C. D. Cole, R. J. Hendershoot, M. Cotten, T. A. Cross, and D. D. Busath. 1999. Non-contact dipole effects on channel permeation. III. Anomalous proton conductance effects in gramicidin. *Biophys. J.* 77:2492–2501.

Pomès, R. 1999. Theoretical studies of the Grotthuss mechanism in biological proton wires. *Isr. J. Chem.* 39:387–395.

Pomès, R., and B. Roux. 1996a. Theoretical study of H^+ translocation along a model proton wire. *J. Phys. Chem.* 100:2519–2527.

Pomès, R., and B. Roux. 1996b. Structure and dynamics of a proton wire: a theoretical study of H^+ translocation along the single-file water chain in the gramicidin A channel. *Biophys. J.* 71:19–39.

Pomès, R., and B. Roux. 1998. Free energy profiles for H^+ conduction along hydrogen-bonded chains of water molecules. *Biophys. J.* 75: 33–40.

Quigley, E. P., A. Emerick, D. S. Crumrine, and S. Cukierman. 1998. Proton current attenuation by methanol in a dioxolane-linked gramicidin A dimer in different lipid bilayers. *Biophys. J.* 5:2811–2820.

Quigley, E. P., P. Quigley, D. S. Crumrine, and S. Cukierman. 1999. Proton conduction in different stereoisomers of the dioxolane linked gramicidin A. *Biophys. J.* 77:2479–2491.

Riistma, S., G. Hummer, A. Puustinem, R. B. Dyer, W. H. Woodruff, and M. Wilkström. 1997. Bound water in the proton translocation mechanism of the heme-copper oxidases. *FEBS Lett.* 414:275–280.

Robinson, R. A., and R. H. Stokes. 1959. Electrolyte Solutions, 2nd Ed. Butterworths, London.

Sansom, M. S. P., I. D. Kerr, J. Breed, and R. Sankararamakrishnan. 1996. Water in channel-like cavities: structure and dynamics. *Biophys. J.* 70:693–702.

Sarges, R., and B. Witkop. 1965. V. The structure of valine- and isoleucine-gramicidin A. *J. Am. Chem. Soc.* 87:2011–2019.

Schumaker, M. F., R. Pomès, and B. Roux. 1999. A combined molecular dynamics and diffusion model of single proton-conduction through gramicidin. *Biophys. J.* 76:A442 (Abstr.).

Schumaker, M. F., R. Pomès, and B. Roux. 2000a. A combined molecular dynamics and diffusion model of single proton conduction through gramicidin. *Biophys. J.* (submitted).

Schumaker, M. F., R. Pomès, B. Roux, and S. Cukierman. 2000b. New experimental results and an extended model of proton conduction through gramicidin. *Biophys. J.* 78:348A (Abstr.).

Stankovic, C. J., S. H. Heinemann, J. M. Delfino, F. J. Sigworth, and S. L. Schreiber. 1989. Transmembrane channels based on tartaric acid-gramicidin A hybrids. *Science.* 244:813–817.

Tuckerman, M., K. Laasonen, M. Sprik, and M. Parrinello. 1995. *Ab initio* molecular dynamics simulation of the solvation and transport of H_3O^+ and OH^- ions in water. *J. Phys. Chem.* 99:5749–5752.

Vuilleumier, R., and D. Borgis. 1998. Quantum dynamics of an excess proton in water using an extended empirical valence-bond Hamiltonian. *J. Phys. Chem.* 102:4261–4264.

Vuilleumier, R., and D. Borgis. 1999. Transport and spectroscopy of the hydrated proton: a molecular dynamics study. *J. Chem. Phys.* 111: 4251–4266.